

NEXT: Multi-Grained Mixture of Experts via Text-Modulation for Multi-Modal Object Re-Identification

Shihao Li¹, Aihua Zheng^{1*}, Andong Lu², Jin Tang², Jixin Ma³

¹School of Artificial Intelligence, Anhui University

²School of Computer Science and Technology, Anhui University

³School of Computing and Mathematical Sciences, University of Greenwich

{shli0603, ahzheng214, adlu_a}@foxmail.com, tangjin@ahu.edu.cn, j.ma@greenwich.ac.uk

Abstract

Multi-modal object Re-Identification (ReID) aims to obtain accurate identity features across heterogeneous modalities. However, most existing methods rely on implicit feature fusion modules, making it difficult to model fine-grained recognition patterns under various challenges in real world. Benefiting from the powerful Multi-modal Large Language Models (MLLMs), the object appearances are effectively translated into descriptive captions. In this paper, we propose a reliable caption generation pipeline based on attribute confidence, which significantly reduces the unknown recognition rate of MLLMs and improves the quality of generated text. Additionally, to model diverse identity patterns, we propose a novel ReID framework, named **NEXT**, the Multi-grained Mixture of Experts via Text-Modulation for Multi-modal Object Re-Identification. Specifically, we decouple the recognition problem into semantic and structural branches to separately capture fine-grained appearance features and coarse-grained structure features. For semantic recognition, we first propose a Text-Modulated Semantic Experts (TMSE), which randomly samples high-quality captions to modulate experts capturing semantic features and mining inter-modality complementary cues. Second, to recognize structure features, we propose a Context-Shared Structure Experts (CSSE), which focuses on the holistic object structure and maintains identity structural consistency via a soft routing mechanism. Finally, we propose a Multi-Grained Features Aggregation (MGFA), which adopts a unified fusion strategy to effectively integrate multi-grained experts into the final identity representations. Extensive experiments on four public datasets demonstrate the effectiveness of our method and show that it significantly outperforms existing state-of-the-art methods.

Introduction

Object re-identification (ReID) aims to construct discriminative identity representations by capturing object characteristics such as appearance, clothing, body shape, and posture (Leng, Ye, and Tian 2020; Ye et al. 2022; He et al. 2021; Luo et al. 2019). However, in real world scenarios, variations in illumination, weather, and occlusion (Sun et al. 2018; Lu et al. 2023; Chen et al. 2022) hinder the performance of classical ReID methods. To address these chal-

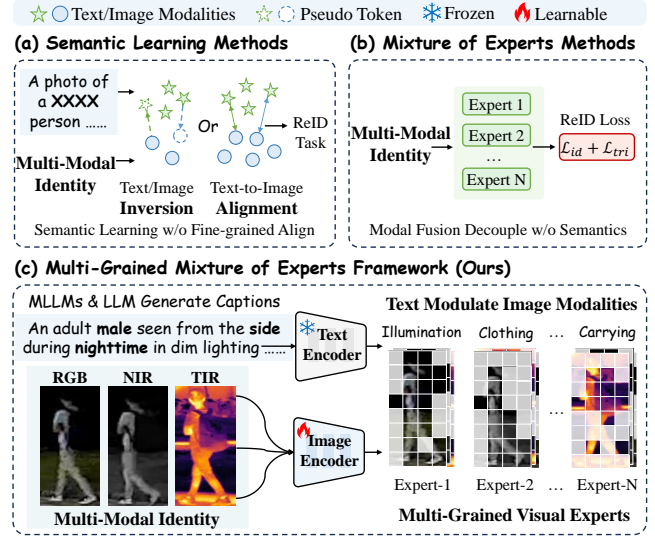


Figure 1: Previous (a) semantic learning methods learn identity prompts via text/image inversion or alignment strategies, which fail to achieve fine-grained alignment. (b) Mixture of experts methods decouple the multi-modal fusion but lack semantic understanding. (c) Our proposed framework modulates image modalities via concrete text captions and decouples appearance and structure into diverse experts.

enges, multi-modal object ReID (Li et al. 2020; Zheng et al. 2023, 2021, 2025) has attracted increasing research interest in recent years. Benefiting from the complementary advantages of diverse spectral modalities, the identity features can be comprehensively captured. Despite this, intra-modal noise and inter-modal heterogeneity remain the key obstacles for effective identity representation fusion. To overcome these issues, existing methods focus on implicit identity-level feature fusion (Wang et al. 2024; Zhang et al. 2025; Wang et al. 2025b,a), fine-grained feature complementarity (Yu et al. 2024; Feng et al. 2025), and frequency-domain interactions (Yang et al. 2025; Zhang et al. 2024). However, semantic-aware fusion (Wang et al. 2025c; Li et al. 2025) of multi-modal identity features is still underexplored.

Recent progress in vision-language models (Hurst et al. 2024; Bai et al. 2023; Liu et al. 2023; Radford et al. 2021;

*Corresponding author (ahzheng214@foxmail.com).

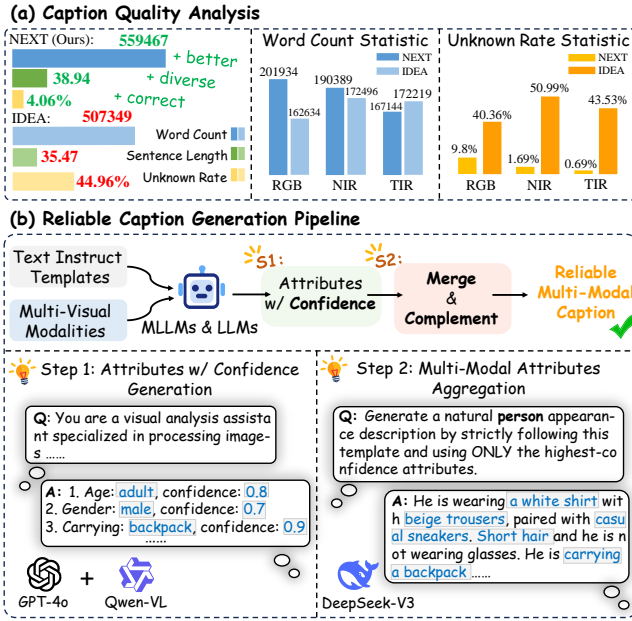


Figure 2: Caption analysis and generation. We first report the word count and the rate of captions containing ‘none,’ ‘unknown,’ or ‘unclear’ words to assess generation quality, and then show the reliable caption generation pipeline with MLLMs.

Li et al. 2022) has advanced visual understanding tasks (Li, Sun, and Li 2023; Yang et al. 2024). Pioneering methods such as IDEA (Wang et al. 2025c), TVI-LFM (Hu, Yang, and Ye 2024), and MP-ReID (Zhai et al. 2024) integrate MLLMs into the ReID tasks by generating identity-relevant captions, thereby extending identity representations into the textual modality. However, low-quality spectral noise and style discrepancies introduce semantic noise and omissions into the text generation process of MLLMs. Information bias during long-context text generation serves as a major cause of hallucinations (Fu et al. 2024) in MLLMs, with longer texts increasing the likelihood of such errors. Additionally, guiding MLLMs to reason the fine-grained attributes across visible and infrared spectra is a highly labor-intensive process. To tackle this, we propose a reliable caption generation framework, as shown in Fig. 2 (b). Specifically, we decompose the caption generation into two steps: confidence-aware attributes generation and multi-modal attributes aggregation. By enforcing the model to output a confidence score for each attribute, we encourage the MLLMs to perform fine-grained evaluation for each attribute. Based on the confidence scores, we quantify the attribute importance across different modalities, enabling us to complement missing semantic information through multi-modal attribute sets.

High-quality captions effectively guide the model to focus on identity-relevant representations. Building on this, we propose a multi-grained mixture of experts framework named NEXT, as shown in Fig. 1 (c), which models the identity recognition process through semantic-sampling and structure-aware experts. The framework consists of three main components: Text-Modulated Semantic Experts

(TMSE), Context-Shared Structure Experts (CSSE), and Multi-Grained Features Aggregation (MGFA). Specifically, TMSE samples part-level fine-grained features within each modality. The text modulation mechanism encourages the experts to focus on semantically relevant regions, thereby capturing intra-modality identity semantic features. Meanwhile, CSSE perceives inter-modality structural features of the object identity through a soft routing mechanism shared across modalities. Finally, MGFA unifies the features of multi-grained experts into a comprehensive identity representation. Extensive experiments on four multi-modal object ReID benchmarks demonstrate the effectiveness of our proposed approach. In summary, our contributions are as follows:

- To obtain accurate object appearance descriptions, we propose a reliable caption generation pipeline that leverages attribute confidence scores to effectively harness MLLMs in producing high-quality textual annotations.
- To model diverse identity patterns, we propose the Text-Modulated Semantic Experts (TMSE) and the Context-Shared Structure Experts (CSSE) to decouple the recognition problem into semantic and structural branches. The Multi-Grained Features Aggregation (MGFA) is proposed to integrate multi-grained experts into a unified identity representation.
- Extensive experiments are conducted on four public benchmarks to validate the effectiveness of our method. The results demonstrate the proposed method significantly outperforms the state-of-the-art methods.

Related Work

Multi-Modal Object Re-Identification

Multi-modal object ReID leverages the complementary imaging advantages of multi-spectra to enable robust identity recognition under adverse conditions. However, intra-modal noise and inter-modal spectral heterogeneity remain significant challenges. To fuse the heterogeneous visual features, TOP-ReID (Wang et al. 2024) proposes a modality permutation and reconstruction mechanism to align multi-modal representations. MambaPro (Wang et al. 2025a) presents a selective state-space fusion approach based on Mamba (Gu and Dao 2023) to aggregate intra- and inter-modal features. EDITOR (Zhang et al. 2024) adopts frequency- and feature-based selection mechanisms to filter out background and low-quality noise. FACENet (Zheng et al. 2025) utilizes illumination priors to enhance degraded modalities. ICPL-ReID (Li et al. 2025) applies an identity prototype-based conditional prompt learning method to guide semantic learning across modalities. IDEA (Wang et al. 2025c) inverts textual features into the visual space to guide model learning, and captures discriminative features across multi-modal via deformable aggregation. Despite these advancements, existing methods still lack a deep exploration of identity semantics and intrinsic structures. To bridge this gap, we propose a multi-grained mixture of experts via text-modulation that fuses features from different modalities through semantic and structural perspectives, aiming to enhance multi-modal identity representation.

Semantic Learning in Re-Identification

Large-scale vision-language foundation models, such as CLIP (Radford et al. 2021), exhibit powerful visual perception and semantic understanding capabilities. Researchers employ the learnable prompt (Zhou et al. 2022b,a) to effectively adapt these models to classification, retrieval, and open-set recognition tasks. Methods like CLIP-ReID (Li, Sun, and Li 2023) and PromptSG (Yang et al. 2024) utilize learnable semantic prompts to transfer the CLIP (Radford et al. 2021) model to object ReID tasks. The rise of MLLMs (Hurst et al. 2024; Bai et al. 2023; Liu et al. 2023) significantly advances visual understanding tasks. Numerous studies demonstrate the effectiveness of MLLMs (Dai et al. 2023; Liu et al. 2024b) in generating high-quality text and robust generalization in vision-language alignment. Other approaches, such as MP-ReID (Zhai et al. 2024), TVI-LFM (Hu, Yang, and Ye 2024), and IDEA (Wang et al. 2025c), exploit MLLMs to generate identity-level textual descriptions from existing ReID datasets. However, these methods still lack reliable text generation under multi-modal conditions. Unlike existing method (Wang et al. 2025c), we further quantify attributes and propose a confidence-aware attribute generation strategy. We incorporate a multi-modal merging and complementation mechanism to achieve high-quality and reliable caption generation. Additionally, we introduce the NEXT framework, which leverages semantic experts to extract fine-grained multi-modal features, aiming to tackle diverse semantic challenges in multi-modal scenarios.

Multi-Modal Mixture of Experts

Mixture-of-Experts (MoE) (Jacobs et al. 1991) achieves remarkable progress in both computer vision and natural language processing domains due to its flexible design and efficient activation mechanisms. In multi-modal visual tasks (Wu et al. 2025; Yun et al. 2024; Han et al. 2024), MoE frameworks are typically designed with modality-shared and modality-specific experts to effectively capture diverse multi-modal features. However, these methods still fall short in learning identity-related representations for multi-modal object ReID. DeMo (Wang et al. 2025b) first applies the MoE framework to the multi-modal ReID task by combining modality-specific experts to decouple shared and unique features. MFRNet (Feng et al. 2025) introduces pixel-level feature generation and interaction with sparse MoE to extract discriminative features with minimal parameter overhead. Despite this, these methods lack fine-grained identity semantic understanding. To address this limitation, we propose text-modulated semantic experts and context-shared structure experts to jointly capture semantic and structural features, enabling more comprehensive identity representation of multi-modalities.

Methodology

In this section, we elaborate on the proposed framework, NEXT. Fig. 3 proposes the Multi-Grained Mixture-of-Experts framework that includes Text-Modulated Semantic Experts (TMSE), Context-Shared Structure Experts (CSSE), and Multi-Grained Features Aggregation (MGFA) module.

Reliable Caption Generation

As shown in Fig. 2, we propose the reliable caption generation pipeline, which decomposes caption generation into two steps: attributes generation and attributes aggregation.

Confidence-Aware Attributes Generation. We first define an instruction template to guide multiple MLLMs (e.g., GPT-4o (Hurst et al. 2024), Qwen-VL (Bai et al. 2023), etc.) in structuring the attribute set of the input image. However, simple structured attribute information cannot quantify the confidence level of each item. We introduce the concept of confidence score in the instruction template, as shown in Fig. 2 (b). This allows us to observe the confidence level that each MLLM assigns to attributes.

Multi-Modal Attributes Aggregation. To eliminate attribute disparities across modalities, we design an attribute aggregation rule with lightweight reasoning ability. For the RGB modal, we select the highest-confidence attributes from the NIR and TIR modalities, which are unaffected by lighting conditions, to complement the absent information. Similarly, we apply the same complementary strategy to other modalities to obtain complete and reliable attribute sets. Building on the above complete attribute set, we define the caption generation instruction to guide the LLM (Liu et al. 2024a) to generate the final text captions.

Multi-Modal Features Extraction

Each multi-modal sample includes three modalities: visible light (RGB), near-infrared (NIR), and thermal infrared (TIR), denoted as $\mathbf{X}_I = [X_{I,rgb}, X_{I,nir}, X_{I,tir}]$, along with detailed appearance captions $\mathbf{X}_T = [X_{T,rgb}, X_{T,nir}, X_{T,tir}]$. We feed the visual modality \mathbf{X}_I into the CLIP visual encoder $\mathcal{V}(\cdot)$ to extract visual features $\mathbf{F}_I = [\mathbf{f}_I^{cls}; \mathbf{F}_I^{tok}] \in \mathbb{R}^{3 \times (1+N) \times D}$, and input the appearance description \mathbf{X}_T into the frozen CLIP text encoder $\mathcal{T}(\cdot)$ to extract textual features $\mathbf{F}_T = [\mathbf{f}_T^{cls}; \mathbf{F}_T^{tok}] \in \mathbb{R}^{3 \times (1+L) \times D}$, where N denotes the length of visual patch tokens, L is the length of text patch tokens, D is the dimension length.

Text-Modulated Semantic Experts

In real world, challenges like illumination variations, background noise, and image degradation impact quality of local regions across modalities, making it essential to bridge modality gaps and extract complementary features. However, existing approaches often lack explicit semantic guidance. To address this, we leverage the object-level textual semantics \mathbf{X}_T extracted from MLLMs to guide a set of semantic experts $\mathbf{E}_T = \{E_t^{(1)}, E_t^{(2)}, \dots, E_t^{(N_T)}\}$ in dynamically sampling semantic-related local features across different modalities, to tackle various semantic challenges, where N_T denotes the number of semantic experts. The structure of each expert is defined as:

$$E_t^i(\mathbf{F}) = \text{Dropout}(\text{MLP}(\text{LN}(\mathbf{F}))) + \mathbf{F}, \quad (1)$$

where \mathbf{F} denotes the input features, LN denotes a layer normalization, MLP refers a multilayer perceptron, and Dropout with a rate of 0.1 is applied to prevent overfitting.

Dynamic Sampling Route. To sample semantic features from each modality, we design a set of modality-specific sampling routes for each expert, denoted as $\mathbf{R} =$

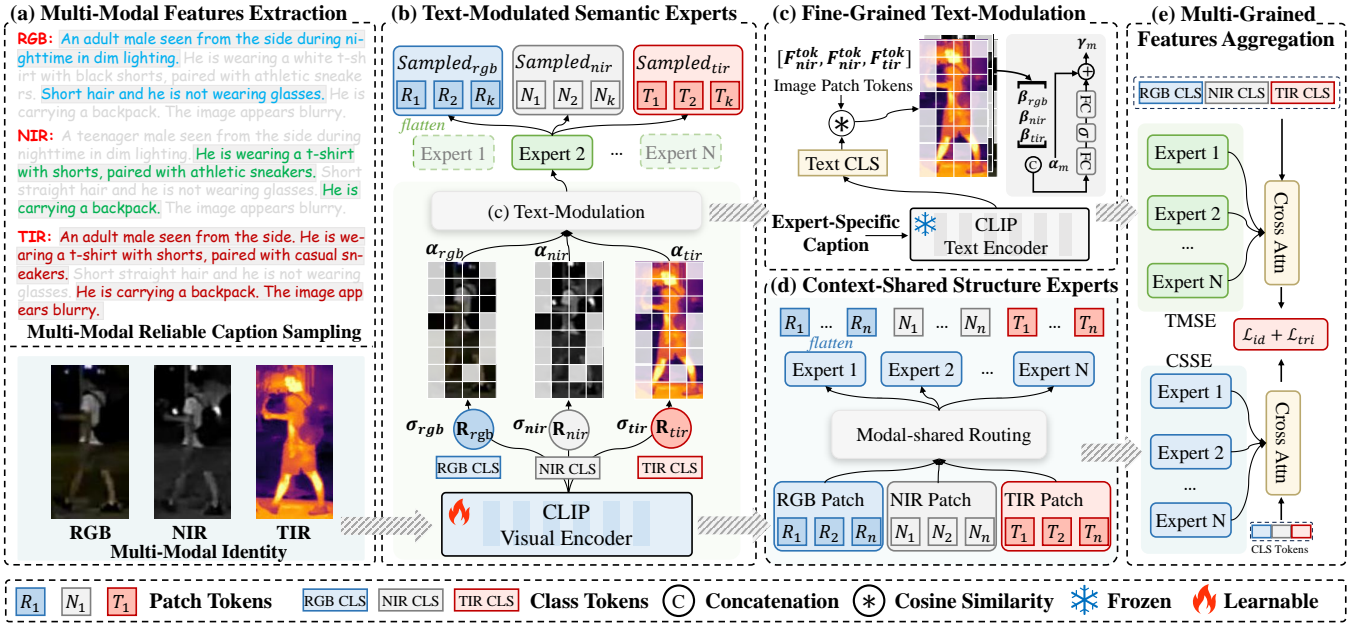


Figure 3: The overview of our proposed framework. First, we divide multi-modal features into (a) reliable caption sampling and multi-modal identity representations. Then, we feed visual modalities into the CLIP visual encoder to obtain visual embeddings, which are passed into both (b) Text-Modulated Semantic Experts (TMSE) and (d) Context-Shared Structure Experts (CSSE), decoupling identity recognition into fine-grained appearance recognition and coarse-grained structure recognition. For TMSE, we input randomly sampled captions into (c) Fine-Grained Text-Modulation to guide the sampling process. Finally, (e) Multi-Grained Features Aggregation (MGFA) efficiently integrates multi-grained expert features to form the final identity representation.

$[R_{rgb}, R_{nir}, R_{tir}]$. We encode the patch-level features $\mathbf{F}_{I,m}^{\text{tok}}$ into the routing matrix α_m , and map the class token $\mathbf{f}_{I,m}^{\text{cls}}$ into the dynamic threshold σ_m as follows:

$$\begin{aligned} \alpha_m &= \text{FC}^2(\delta(\text{FC}^1(\mathbf{F}_{I,m}^{\text{tok}}))), \quad \alpha_m \in \mathbb{R}^{H \times W} \\ \sigma_m &= \text{FC}^2(\delta(\text{FC}^1(\mathbf{f}_{I,m}^{\text{cls}}))), \quad \sigma_m \in \mathbb{R} \end{aligned} \quad (2)$$

where $\text{FC}^1 \in \mathbb{R}^{D \times D}$ and $\text{FC}^2 \in \mathbb{R}^{D \times 1}$ denotes fully connected layer, δ is GELU activation function (Hendrycks and Gimpel 2016), and $m \in \{rgb, nir, tir\}$.

$$\mathbf{M}_m(i, j) = \begin{cases} 1, & \text{if } \alpha_m(i, j) > \sigma_m \\ 0, & \text{otherwise} \end{cases}, \quad (3)$$

As formulated in Eq. (3), we assign 1 to entries in α_m that exceed the threshold σ_m and 0 otherwise, to discard irrelevant features while keeping the operation differentiable.

Fine-Grained Text Modulation. To empower the semantic awareness of each expert, we employ random semantic text prompts during training, guiding each expert toward distinct semantic challenges. Formally, the raw semantic text is decomposed into fine-grained sentences for each modality: $X_{T,m} = \{s_m^{(1)}, s_m^{(2)}, \dots, s_m^{(n_m)}\}$, where n_m is the maximum number of sentences. For each expert $E_t^{(i)}$, we randomly select a subset $\hat{X}_{T,m}^{(i)}$ from $X_{T,m}$ as its modulation signal. The sampling process is defined as:

$$\begin{aligned} \hat{\mathbf{X}}_T^{(i)} &= [\hat{X}_{T,rgb}^{(i)}, \hat{X}_{T,nir}^{(i)}, \hat{X}_{T,tir}^{(i)}], \\ \hat{X}_{T,m}^{(i)} &\sim \text{Sampling}(X_{T,m}), \end{aligned} \quad (4)$$

where i denotes the i -th semantic experts, and **Sampling** is a random probability distribution.

To modulate the sampling route, we first encode the randomly sampled high-quality semantic text into the visual-text latent space as text feature vector $\mathbf{f}_{T,m}^{\text{cls}}$. Second, we compute the cosine similarity between this text vector and the visual patch tokens to obtain the semantic matrix β_m :

$$\beta_m = \frac{\mathbf{f}_{T,m}^{\text{cls}} \cdot \mathbf{F}_{I,m}^{\text{tok}}}{\|\mathbf{f}_{T,m}^{\text{cls}}\|_2 \cdot \|\mathbf{F}_{I,m}^{\text{tok}}\|_2}, \quad \beta_m \in \mathbb{R}^{H \times W} \quad (5)$$

where $\|\cdot\|_2$ means L_2 normalization. We then integrate this semantic guidance with the route matrix α_m to produce the modulation matrix γ_m :

$$\gamma_m = \text{FC}^4(\delta(\text{FC}^3(\alpha_m, \beta_m))) + \alpha_m, \quad \gamma_m \in \mathbb{R}^{H \times W} \quad (6)$$

where $\text{FC}^3 \in \mathbb{R}^{2 \times D/2}$ and $\text{FC}^4 \in \mathbb{R}^{D/2 \times 1}$ denotes the fully connected layer within the modulation network whose structure is illustrated in Fig. 3 (c).

Finally, we replace the route matrix α_m in Eq. (3) with the modulated matrix γ_m to obtain the final modulation-based sampling matrix $\hat{\mathbf{M}}_m$.

$$\hat{\mathbf{F}}_{I,m}^{\text{tok}} = E_t(\mathbf{F}_{I,m}^{\text{tok}}), \quad \hat{\mathbf{F}}_I = \text{Concat}(\hat{\mathbf{M}}_m \odot \hat{\mathbf{F}}_{I,m}^{\text{tok}}), \quad (7)$$

According to Eq. (7) above, $\hat{\mathbf{M}}_m$ dynamically samples the informative features for each semantic expert $E_t^{(i)}$ within a

modality. These sampled features are concatenated to obtain the final multi-modal semantic feature $\hat{\mathbf{F}}_I$.

Context-Shared Structure Experts

Although semantic experts focus on fine-grained part sampling under various semantic challenges. The identity recognition and discrimination still rely on the structural integrity of the object. To this end, we introduce a set of structure experts, denoted as $\mathbf{E}_C = \{E_c^{(1)}, E_c^{(2)}, \dots, E_c^{(N_C)}\}$, to comprehensively perceive the holistic object structure across modalities, where N_C denotes the number of structure experts and $E_c^{(i)}$ shares the same architecture as $E_t^{(i)}$ in Eq. 1.

Specifically, to preserve structural integrity, we first concatenate multi-modal patch features as $\mathbf{F}_I^{\text{tok}} = [\mathbf{F}_{I,rgb}^{\text{tok}}, \mathbf{F}_{I,nir}^{\text{tok}}, \mathbf{F}_{I,tir}^{\text{tok}}]$, and then feed them into a modality-shared routing network \mathbf{R}_s to compute the expert fusion weights as follows:

$$\omega = \text{Softmax}(\text{FC}(\mathbf{F}_I^{\text{tok}})), \quad \omega \in \mathbb{R}^{N_C} \quad (8)$$

where **Softmax** encodes the expert selection weights, resulting in the soft routing matrix ω .

Finally, we feed the concatenated multi-modal token features into the structure experts \mathbf{E}_C and compute the final multi-modal structural representation by weighting each output of expert using the soft routing matrix ω . The process is formulated as follows:

$$\begin{aligned} \tilde{\mathbf{F}}_I &= \sum_{i=1}^{N_C} \omega_i \cdot E_c^{(i)}(\mathbf{F}_I^{\text{tok}}), \\ \tilde{\mathbf{F}}_I^{\text{tok}} &= \left\{ E_c^{(i)}(\mathbf{F}_I^{\text{tok}}) \mid i = 1, 2, \dots, N_C \right\}, \end{aligned} \quad (9)$$

where $\tilde{\mathbf{F}}_I$ represents the final multi-modal structure feature.

Multi-Grained Features Aggregation

Experts of different types mine various identity features. The semantic expert E_T extracts fine-grained semantic features $\hat{\mathbf{F}}_I^{(i)}$, and the structural expert E_C captures structural consistency features $\tilde{\mathbf{F}}_I$. As illustrated in Fig. 3 (e), we combine these features to form the complete object identity feature set $\mathbf{F}_I^{\text{exp}} = [\hat{\mathbf{F}}_I^{(1)}, \hat{\mathbf{F}}_I^{(2)}, \dots, \hat{\mathbf{F}}_I^{(N_T)}; \tilde{\mathbf{F}}_I]$. The modality class tokens are concatenated to form the modality query features $\mathbf{f}_I^{\text{cls}} = [\mathbf{f}_{I,rgb}^{\text{cls}}, \mathbf{f}_{I,nir}^{\text{cls}}, \mathbf{f}_{I,tir}^{\text{cls}}]$. Following this, we treat $\mathbf{f}_I^{\text{cls}}$ as the query feature Q and the expert features as the key K and value V . Through the Cross-Attention mechanism, we obtain the multi-modal representation for each expert and average them to form the final identity representation $\hat{\mathbf{f}}_I^{\text{cls}}$. The process is formulated as follows:

$$\hat{\mathbf{f}}_I^{\text{cls}} = \text{Average}(\hat{\mathbf{f}}_I^{\text{cls}(1)}, \hat{\mathbf{f}}_I^{\text{cls}(2)}, \dots, \hat{\mathbf{f}}_I^{\text{cls}(N_T)}; \tilde{\mathbf{f}}_I^{\text{cls}}), \quad (10)$$

$$\begin{aligned} \hat{\mathbf{f}}_I^{\text{cls}(i)} &= \text{FFN}(\text{LN}(\text{CA}(\mathbf{f}_I^{\text{cls}}, \mathbf{F}_I^{\text{exp}(i)}))), \\ &\text{for } i = 1, \dots, N_T + 1 \end{aligned} \quad (11)$$

where **CA** is the Cross-Attention mechanism, and **FFN** is the feedback forward layer.

Optimization and Inference

In line with prior work (He et al. 2021; Luo et al. 2019), we use the object identity ID label as the ground-truth to train the classification loss L_{id} , and adopt the triplet loss L_{tri} to enhance identity compactness and separability. The final loss function is defined as:

$$L_{\text{final}}(\hat{\mathbf{f}}_I^{\text{cls}}) = L_{\text{id}}(\hat{\mathbf{f}}_I^{\text{cls}}) + L_{\text{tri}}(\hat{\mathbf{f}}_I^{\text{cls}}). \quad (12)$$

During inference, the fused feature serves as the final object representation for multi-modal retrieval.

Experiment

Datasets and Evaluation Protocols

Datasets. We evaluate our method on four multi-modal object ReID datasets: RGBNT201 (Zheng et al. 2021), MSVR310 (Zheng et al. 2023), RGBNT100 (Li et al. 2020), and WMVEID863 (Zheng et al. 2025). To extend these datasets, we employ GPT-4o (Hurst et al. 2024) and Qwen-VL (Bai et al. 2023) to automatically generate object attribute with confidence, and DeepSeek-V3 (Liu et al. 2024a) to compose the final caption for each image modality.

Evaluation Protocols. In line with the convention of community (He et al. 2021; Ye et al. 2022), we use Rank-K ($K = 1, 5, 10$) matching accuracy and the Mean Average Precision (mAP) as evaluation metrics. As in previous works (Zheng et al. 2021; Li et al. 2020; Zheng et al. 2025), we adopt the common evaluation protocol for RGBNT201 (Zheng et al. 2021), RGBNT100 (Li et al. 2020) and WMVEID863 (Zheng et al. 2025). For MSVR310 (Zheng et al. 2023), we filter out samples with the same identity and time span based on time labels to avoid easy matching (Zheng et al. 2023).

Comparison with State-of-the-Art Methods

Performance on Person Dataset. In Tab. 1, we compare our NEXT with existing methods on the RGBNT201 dataset. Benefiting from the flexible fusion of semantic and structural experts, our method achieves a significant performance lead, reaching 82.4%/86.6% mAP/Rank-1 accuracy. Compared with DeMo, which adopts the MoE structure to handle modality-shared and specific features, our method demonstrates superior performance by perceiving both the semantic and structural features of the objects. Against IDEA, which utilizes semantic inversion and deformable offset sampling, our method leverages text-modulation to guide expert sampling multi-modal semantics, improving mAP and Rank-1 by +2.2% and +4.5%, respectively. These results validate the effectiveness of NEXT in learning discriminative multi-modal identity features via textual semantics.

Performance on Vehicle Dataset. Tab. 1 outlines the performance of our method on vehicle ReID datasets. On the MSVR310 dataset, our approach significantly outperforms existing methods, achieving 60.8%/79.0% mAP/Rank-1 accuracy, attributed to its semantic sampling and structural perception. On the RGBNT100 dataset, our method continues to lead in mAP performance. For the challenging WMVEID863 dataset, where lighting variations degrade recognition performance, our method still improves over

Methods	RGBNT201				MSVR310		RGBNT100		WMVEID863			
	mAP	R-1	R-5	R-10	mAP	R-1	mAP	R-1	mAP	R-1	R-5	R-10
HAMNet (Li et al. 2020)	27.7	26.3	41.5	51.7	27.1	42.3	74.5	93.3	45.6	48.5	63.1	68.8
PFNet (Zheng et al. 2021)	38.5	38.9	52.0	58.4	23.5	37.4	68.1	94.1	50.1	55.9	68.7	75.1
IEEE (Wang et al. 2022)	46.4	47.1	58.5	64.2	21.0	41.0	61.3	87.8	45.9	48.6	64.3	67.9
CCNet (Zheng et al. 2023)	-	-	-	-	36.4	55.2	77.2	96.3	50.3	52.7	69.6	75.1
TOP-ReID (Wang et al. 2024)	72.3	76.6	84.7	89.4	35.9	44.6	81.2	96.4	67.7	75.3	80.8	83.5
FACENet (Zheng et al. 2025)	-	-	-	-	36.2	54.1	81.5	96.9	<u>69.8</u>	77.0	81.0	84.2
EDITOR (Zhang et al. 2024)	66.5	68.3	81.1	88.2	39.0	49.3	82.1	96.4	65.6	73.8	80.0	82.3
ICPL-ReID (Li et al. 2025)	75.1	77.4	84.2	87.9	<u>56.9</u>	<u>77.7</u>	87.0	98.6	67.2	74.0	81.3	<u>85.6</u>
MambaPro (Wang et al. 2025a)	78.9	83.4	89.8	91.9	47.0	56.5	83.9	94.7	69.5	76.9	80.6	83.8
PromptMA (Zhang et al. 2025)	78.4	80.9	87.0	88.9	55.2	64.5	85.3	97.4	-	-	-	-
DeMo (Wang et al. 2025b)	79.0	82.3	88.8	92.0	49.2	59.8	86.2	97.6	68.8	<u>77.2</u>	<u>81.5</u>	83.8
IDEA (Wang et al. 2025c)	80.2	82.1	90.0	93.3	47.0	62.4	<u>87.2</u>	96.5	-	-	-	-
MFRNet (Feng et al. 2025)	<u>80.7</u>	<u>83.6</u>	<u>91.9</u>	<u>94.1</u>	50.6	64.8	88.2	97.4	-	-	-	-
NEXT(Ours)	82.4	86.6	92.0	94.7	60.8	79.0	88.2	<u>97.7</u>	70.9	77.8	84.3	86.7

Table 1: Comparison with the state-of-the-art methods on four benchmarks: RGBNT201, MSVR310, RGBNT100, and WMVEID863. The best and second best results are marked in **bold** and underline, respectively.

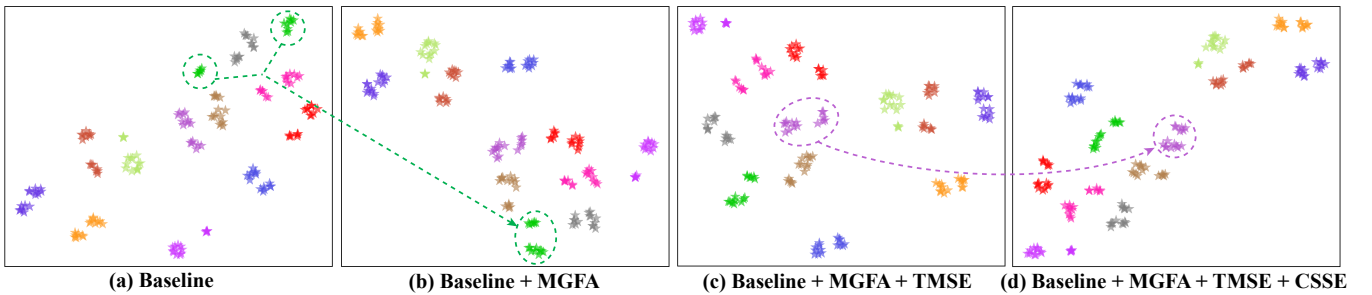


Figure 4: T-SNE (Van der Maaten and Hinton 2008) visualization of the feature distribution on RGBNT201 (a) Baseline, (b) Baseline + MGFA, (c) Baseline + MGFA + TMSE, and (d) Baseline + MGFA + TMSE + CSSE (Ours).

Index	Modules			Metrics		Params	Flops
	MGFA	TMSE	CSSE	mAP	R-1	M	G
A	✗	✗	✗	71.0	73.6	88.3	33.3
B	✓	✗	✗	74.2	76.6	88.5	33.5
C	✓	✓	✗	78.9	84.4	92.5	43.7
D	✓	✓	✓	82.4	86.6	94.8	44.8

Table 2: Ablation studies of different modules.

Index	Methods	Metrics		Params	Flops
		mAP	R-1	M	G
A	All-Token	79.0	83.0	94.8	43.9
B	Top- K	81.4	84.3	94.8	44.8
C	Fixed- σ	80.3	85.0	94.8	44.8
D	σ_m (Ours)	82.4	86.6	94.8	44.8

Table 3: Effectiveness of sampling strategies.

FACENet by +1.1%/+0.8% mAP/Rank-1. These results confirm the strong generalization and robustness of NEXT in vehicle ReID under complex conditions.

Ablation Studies

On the RGBNT201 dataset, we start from a baseline built on a three-branch CLIP visual encoder, and incrementally incorporate our components to evaluate their specific contributions to the model’s overall performance.

Effectiveness of Key Modules. As shown in Tab. 2, the baseline (Row A) achieves 71.0%/73.6% mAP/Rank-1. In Row B, the MGFA improves performance by +3.2%/+3.0% by fusing baseline features as a single expert. Adding the TMSE module in Row C boosts accuracy to 78.9% mAP and 84.4% Rank-1 under semantic modulation. With the CSSE in Row D, the model gains performance +2.5%/+2.2% in mAP/Rank-1. These results confirm the contribution of each module to the overall performance.

Caption Type	Quality	IDEA		NEXT (Ours)	
		mAP	R-1	mAP	R-1
IDEA-Text	100%	80.2	82.1	80.5	84.7
	35%	76.1	77.9	77.1	79.7
NEXT-Text	70%	78.1	79.9	80.0	82.2
	100%	80.2	84.0	82.4	86.6

Table 4: Effectiveness of caption type and quality for IDEA and our method.

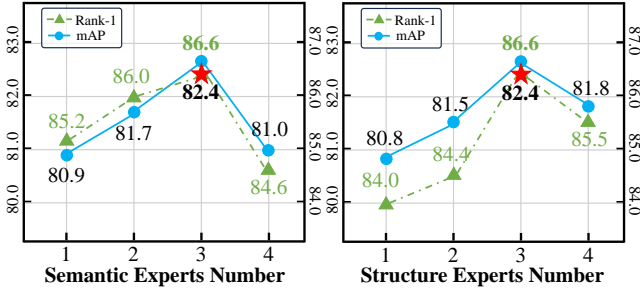


Figure 5: Effectiveness of the number of experts.

Effectiveness of Sampling Strategies. Tab. 3 compares different semantic sampling strategies on RGBNT201. In Row A, the All-Token strategy encodes all patch tokens $\mathbf{F}_{l,m}^{\text{tok}}$, but fails to identify key semantic regions, resulting in significant performance degradation. Row B adopts the Top- K strategy, replacing the dynamic routing threshold σ_m in \mathbf{R}_m with the top 50% tokens, achieving a suboptimal result. Row C replaces the σ_m with a Fixed- σ , which lacks adaptive perception and relies on handcrafted heuristics, leading to inferior performance. In contrast, our dynamic sampling strategy achieves optimal performance, confirming its effectiveness.

Effectiveness of Caption Quality. Tab. 4 shows the impact of text quality on model performance by adding varying levels of noise. Our high-quality captions improve the Rank-1 accuracy of IDEA, while using IDEA’s captions in our model causes a 1.9% drop in both mAP and Rank-1. As caption quality degrades to 70%, performance declines notably. At 35% quality, IDEA and NEXT drop to 76.1%/77.9% and 77.1%/79.7%, respectively. These results confirm that semantic-guided methods strongly rely on high-quality text.

Effectiveness of Experts Number. Fig. 5 illustrates the influences of the number of experts on model performance. With few experts, the model struggles to learn rich semantic information or recognize structural identity cues, which hampers overall performance. Conversely, an excessive number of experts causes redundancy and ambiguity in semantic-structural fusion, impairing identity representation. The results suggest that a moderate number of experts offers the best trade-off and leads to optimal performance.

Visualization Analysis

Feature Distribution. Fig. 4 visualizes feature distributions on RGBNT201 using T-SNE. Comparing Fig. 4 (a) and (b), the introduction of MGFA effectively aggregates different

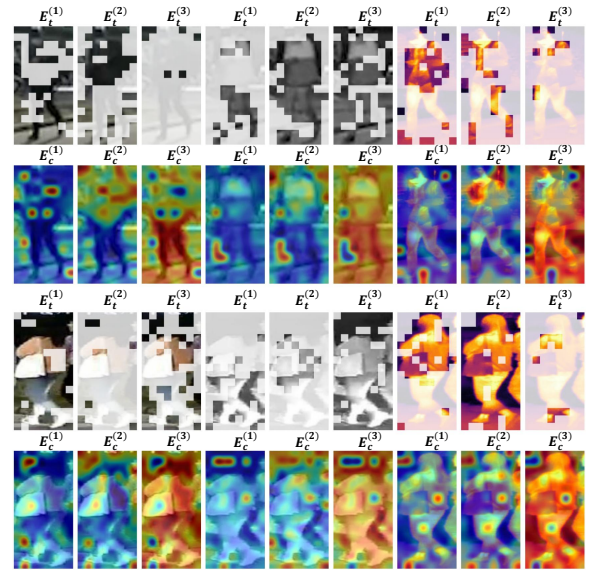


Figure 6: Visualization of the sampled patch tokens and activated feature regions for experts.

instances of the same identity. In Fig. 4 (c), incorporating the TMSE semantic experts improves the separability of samples across identities. In Fig. 4 (d), the inclusion of CSSE structural experts leads to tighter clustering of hard samples, resulting in well-separated intra-class and inter-class distributions. These results validate the effectiveness of each proposed module.

Expert Feature Visualization. Fig. 6 shows that semantic experts focus on different modalities (RGB, NIR, TIR), enabling complementary feature sampling. Structural experts preserve identity structure, with missing parts in one expert compensated by others. These results confirm that NEXT effectively separates semantic and structural modeling for identity recognition.

Conclusion

In this paper, we focus on the semantic learning of multi-modal object ReID. We first propose a reliable multi-modal caption generation pipeline based on MLLMs, which use confidence-aware attribute instruction to construct structured attribute sets, and merge multi-modal attributes to compose high-quality captions. Additionally, we propose the NEXT, a novel multi-grained MoE network for multi-modal ReID. Specifically, we propose the Text-Modulated Semantic Experts (TMSE) and the Context-Shared Structure Experts (CSSE) to decouple the recognition problem into fine-grained semantic sampling and coarse-grained structural perception. Finally, we incorporate a Multi-Grained Features Aggregation (MGFA) module to unify features from multi-grained experts and obtain complete identity representations. Extensive experiments on four popular benchmarks demonstrate the effectiveness of our method. In future work, we plan to continue exploring the powerful role of MLLMs, such as semantic reasoning, for multi-modal object ReID.

References

- Bai, J.; Bai, S.; Yang, S.; Wang, S.; Tan, S.; Wang, P.; Lin, J.; Zhou, C.; and Zhou, J. 2023. Qwen-VL: A Versatile Vision-Language Model for Understanding, Localization, Text Reading, and Beyond. *arXiv:2308.12966*.
- Chen, W.; Chen, I.; Yeh, C.; Yang, H.; Ding, J.; and Kuo, S. 2022. SJDL-Vehicle: Semi-supervised Joint Defogging Learning for Foggy Vehicle Re-identification. In *AAAI*, volume 36, 347–355.
- Dai, W.; Li, J.; Li, D.; Tiong, A. M. H.; Zhao, J.; Wang, W.; Li, B.; Fung, P.; and Hoi, S. C. H. 2023. InstructBLIP: Towards General-purpose Vision-Language Models with Instruction Tuning. In *NeurIPS*.
- Feng, Y.; Li, J.; Xie, C.; Tan, L.; and Ji, J. 2025. Multi-Modal Object Re-identification via Sparse Mixture-of-Experts. In *ICML*.
- Fu, Y.; Xie, R.; Sun, X.; Kang, Z.; and Li, X. 2024. Mitigating hallucination in multimodal large language model via hallucination-targeted direct preference optimization. *arXiv preprint arXiv:2411.10436*.
- Gu, A.; and Dao, T. 2023. Mamba: Linear-Time Sequence Modeling with Selective State Spaces. *arXiv preprint arXiv:2312.00752*.
- Han, X.; Nguyen, H.; Harris, C.; Ho, N.; and Saria, S. 2024. FuseMoE: Mixture-of-Experts Transformers for Fleximodal Fusion. In *NeurIPS*.
- He, S.; Luo, H.; Wang, P.; Wang, F.; Li, H.; and Jiang, W. 2021. TransReID: Transformer-based Object Re-Identification. In *ICCV*, 14993–15002.
- Hendrycks, D.; and Gimpel, K. 2016. Gaussian error linear units (gelus). *arXiv preprint arXiv:1606.08415*.
- Hu, Z.; Yang, B.; and Ye, M. 2024. Empowering Visible-Infrared Person Re-Identification with Large Foundation Models. In *NeurIPS*.
- Hurst, A.; Lerer, A.; Goucher, A. P.; Perelman, A.; Ramesh, A.; Clark, A.; Ostrow, A.; Welihinda, A.; Hayes, A.; Radford, A.; et al. 2024. Gpt-4o system card. *arXiv preprint arXiv:2410.21276*.
- Jacobs, R. A.; Jordan, M. I.; Nowlan, S. J.; and Hinton, G. E. 1991. Adaptive Mixtures of Local Experts. *Neural Comput.*, 3(1): 79–87.
- Kingma, D. P.; and Ba, J. 2014. Adam: A method for stochastic optimization. *arXiv preprint arXiv:1412.6980*.
- Leng, Q.; Ye, M.; and Tian, Q. 2020. A Survey of Open-World Person Re-Identification. *IEEE TCSVT*, 30(4): 1092–1108.
- Li, H.; Li, C.; Zhu, X.; Zheng, A.; and Luo, B. 2020. Multi-Spectral Vehicle Re-Identification: A Challenge. In *AAAI*, 11345–11353.
- Li, J.; Li, D.; Xiong, C.; and Hoi, S. C. H. 2022. BLIP: Bootstrapping Language-Image Pre-training for Unified Vision-Language Understanding and Generation. In *ICML*, volume 162, 12888–12900.
- Li, S.; Sun, L.; and Li, Q. 2023. CLIP-ReID: Exploiting Vision-Language Model for Image Re-identification without Concrete Text Labels. In *AAAI*, 1405–1413.
- Li, S.; Zheng, A.; Li, C.; Tang, J.; and Luo, B. 2025. ICPL-ReID: Identity-Conditional Prompt Learning for Multi-Spectral Object Re-Identification. *IEEE TMM*.
- Liu, A.; Feng, B.; Xue, B.; Wang, B.; Wu, B.; Lu, C.; Zhao, C.; Deng, C.; Zhang, C.; Ruan, C.; et al. 2024a. Deepseek-v3 technical report. *arXiv preprint arXiv:2412.19437*.
- Liu, H.; Li, C.; Wu, Q.; and Lee, Y. J. 2023. Visual Instruction Tuning. In *NeurIPS*.
- Liu, Y.; Chen, P.; Cai, J.; Jiang, X.; Hu, Y.; Yao, J.; Wang, Y.; and Xie, W. 2024b. LamRA: Large Multimodal Model as Your Advanced Retrieval Assistant. *abs/2412.01720*.
- Lu, A.; Zhang, Z.; Huang, Y.; Zhang, Y.; Li, C.; Tang, J.; and Wang, L. 2023. Illumination Distillation Framework for Nighttime Person Re-Identification and a New Benchmark. *IEEE TMM*, 1–14.
- Luo, H.; Gu, Y.; Liao, X.; Lai, S.; and Jiang, W. 2019. Bag of Tricks and a Strong Baseline for Deep Person Re-Identification. In *CVPRW*, 1487–1495.
- Radford, A.; Kim, J. W.; Hallacy, C.; Ramesh, A.; Goh, G.; Agarwal, S.; Sastry, G.; Askell, A.; Mishkin, P.; Clark, J.; Krueger, G.; and Sutskever, I. 2021. Learning Transferable Visual Models From Natural Language Supervision. In *ICML*, volume 139, 8748–8763.
- Sun, Y.; Zheng, L.; Yang, Y.; Tian, Q.; and Wang, S. 2018. Beyond Part Models: Person Retrieval with Refined Part Pooling (and A Strong Convolutional Baseline). In *ECCV*, 480–496.
- Van der Maaten, L.; and Hinton, G. 2008. Visualizing data using t-SNE. *Journal of machine learning research*, 9(11).
- Wang, Y.; Liu, X.; Yan, T.; Liu, Y.; Zheng, A.; Zhang, P.; and Lu, H. 2025a. MambaPro: Multi-Modal Object Re-Identification with Mamba Aggregation and Synergistic Prompt. In *AAAI*.
- Wang, Y.; Liu, X.; Zhang, P.; Lu, H.; Tu, Z.; and Lu, H. 2024. TOP-ReID: Multi-Spectral Object Re-identification with Token Permutation. In *AAAI*, 5758–5766.
- Wang, Y.; Liu, Y.; Zheng, A.; and Zhang, P. 2025b. DeMo: Decoupled Feature-Based Mixture of Experts for Multi-Modal Object Re-Identification. In *AAAI*.
- Wang, Y.; Lv, Y.; Zhang, P.; and Lu, H. 2025c. IDEA: Inverted Text with Cooperative Deformable Aggregation for Multi-modal Object Re-Identification. In *CVPR*, 29701–29710.
- Wang, Z.; Li, C.; Zheng, A.; He, R.; and Tang, J. 2022. Interact, Embed, and Enlarge: Boosting Modality-Specific Representations for Multi-Modal Person Re-identification. In *AAAI*, 2633–2641.
- Wu, C.; Shuai, Z.; Tang, Z.; Wang, L.; and Shen, L. 2025. Dynamic Modeling of Patients, Modalities and Tasks via Multi-modal Multi-task Mixture of Experts. In *ICLR*.
- Yang, X.; Dong, W.; Cheng, D.; Wang, N.; and Gao, X. 2025. TIENet: A Tri-Interaction Enhancement Network for Multimodal Person Reidentification. *IEEE TNNLS*.
- Yang, Z.; Wu, D.; Wu, C.; Lin, Z.; Gu, J.; and Wang, W. 2024. A Pedestrian is Worth One Prompt: Towards Language Guidance Person Re-Identification. In *CVPR*, 17343–17353.

Ye, M.; Shen, J.; Lin, G.; Xiang, T.; Shao, L.; and Hoi, S. C. H. 2022. Deep Learning for Person Re-Identification: A Survey and Outlook. *IEEE TPAMI*, 44(6): 2872–2893.

Yu, Z.; Huang, Z.; Hou, M.; Pei, J.; Yan, Y.; Liu, Y.; and Sun, D. 2024. Representation Selective Coupling via Token Sparsification for Multi-Spectral Object Re-Identification. *IEEE TCSVT*.

Yun, S.; Choi, I.; Peng, J.; Wu, Y.; Bao, J.; Zhang, Q.; Xin, J.; Long, Q.; and Chen, T. 2024. Flex-MoE: Modeling Arbitrary Modality Combination via the Flexible Mixture-of-Experts. In *NeurIPS*.

Zhai, Y.; Zeng, Y.; Huang, Z.; Qin, Z.; Jin, X.; and Cao, D. 2024. Multi-prompts learning with cross-modal alignment for attribute-based person re-identification. In *AAAI*, 6979–6987.

Zhang, P.; Wang, Y.; Liu, Y.; Tu, Z.; and Lu, H. 2024. Magic tokens: Select diverse tokens for multi-modal object re-identification. In *CVPR*, 17117–17126.

Zhang, S.; Luo, W.; Cheng, D.; Xing, Y.; Liang, G.; Wang, P.; and Zhang, Y. 2025. Prompt-Based Modality Alignment for Effective Multi-Modal Object Re-Identification. *IEEE TIP*, 34: 2450–2462.

Zheng, A.; Ma, Z.; Sun, Y.; Wang, Z.; Li, C.; and Tang, J. 2025. Flare-aware cross-modal enhancement network for multi-spectral vehicle Re-identification. *INFFUS*, 116: 102800.

Zheng, A.; Wang, Z.; Chen, Z.; Li, C.; and Tang, J. 2021. Robust Multi-Modality Person Re-identification. In *AAAI*, 3529–3537.

Zheng, A.; Zhu, X.; Ma, Z.; Li, C.; Tang, J.; and Ma, J. 2023. Cross-directional consistency network with adaptive layer normalization for multi-spectral vehicle re-identification and a high-quality benchmark. *INFFUS*, 100: 101901.

Zhong, Z.; Zheng, L.; Kang, G.; Li, S.; and Yang, Y. 2020. Random Erasing Data Augmentation. In *AAAI*, 13001–13008.

Zhou, K.; Yang, J.; Loy, C. C.; and Liu, Z. 2022a. Conditional prompt learning for vision-language models. In *CVPR*, 16816–16825.

Zhou, K.; Yang, J.; Loy, C. C.; and Liu, Z. 2022b. Learning to Prompt for Vision-Language Models. *IJCV*, 130(9): 2337–2348.

Appendix Overview

The appendix presents more comprehensive analysis and results of our NEXT to facilitate the comparison of subsequent methods. Specifically, the structure is organized as follows:

Sec.A Datasets Scale and Implementation Details:

- Datasets Scale.
- Implementation Details.

Sec.B Ablation Studies:

- Effectiveness of Key Modules on Vehicle Dataset.
- Effectiveness of Route Strategy.
- Training and Inference Efficiency Analysis.

Sec.C Reliable Caption Generation:

- Confidence-aware Attributes Generation.
- Multi-Modal Attributes Aggregation.

Sec.D Visualization Analysis:

- Expert Feature Visualization.
- Retrieval Results.

The source [Code](#) will be released upon acceptance.

A. Datasets Scale and Implementation Details

Datasets Scale

We list the dataset statistics in Tab. 5, including the number of samples, identities, and cameras across these datasets. RGBNT201 (Zheng et al. 2021) focuses on person ReID with four non-overlapping camera views and samples composed of RGB, NIR, and TIR modalities. MSVR310 (Zheng et al. 2023) captures vehicles from eight unique angles over extended durations. RGBNT100 (Li et al. 2020) provides diverse vehicle pairs across three modalities. WMVEID863 (Zheng et al. 2025) constructs the largest multi-modal vehicle dataset with harsh lighting challenges.

Datasets	Object Type	# Samples	# IDs	# Cams
RGBNT201	Person	4,787	201	4
MSVR310	Vehicle	2,087	310	8
RGBNT100	Vehicle	17,250	100	8
WMVEID863	Vehicle	4,709	863	8

Table 5: Statistical analysis of datasets.

Implementation Details

We resize each spectral image to 256×128 for person samples, and 128×256 for vehicle samples. Data augmentation includes random horizontal flipping, padding, cropping, and erasing (Zhong et al. 2020). We utilize the vision and text encoders in CLIP as the backbone, freezing all parameters of the text branch for text semantic projection, and keeping the visual branch fully trainable. Adam (Kingma and Ba 2014) optimizer is used with the learning rate of $3.5e-6$, weight decay of 0.0001, and momentum set to 0.9. All experiments are conducted on one NVIDIA RTX 4090 GPU using the PyTorch framework.

B. Ablation Studies

Effectiveness of Key Modules

As shown in Tab. 6, to thoroughly validate the effectiveness of each proposed module, we conduct ablation studies on the vehicle dataset MSVR310 (Zheng et al. 2023). Additionally, we provide the complete ablation results on the RGBNT201 (Zheng et al. 2021) dataset. In Setting A, we use a three-branch CLIP visual encoder as the baseline, achieving 50.1% mAP and 68.9% Rank-1 accuracy on the vehicle dataset. By introducing the MGFA module, which treats each backbone feature as an independent expert, the performance improves to 55.0% mAP and 73.3% Rank-1. Further adding TMSE semantic experts brings an additional +4.7% mAP and +1.8% Rank-1 improvement. Finally, the CSSE structural experts boost performance to an optimal of 60.8% mAP and 79.0% Rank-1. These results validate the effectiveness and generalizability of each proposed component.

Effectiveness of Routing Strategy

As shown in Tab. 8, using shared routing for either E_T or E_C leads to consistent performance gains. In particular, when E_T uses modality-specific routers while E_C uses a shared router (Setting D), the model achieves the best results, with 82.4% mAP and 86.6% Rank-1 accuracy. This indicates that modality-specific semantic routing and shared content routing can effectively balance discrimination and generalization.

Training and Inference Efficiency Analysis

Tab. 7 compares the efficiency of various methods on the RGBNT201 dataset in terms of learnable parameters, FLOPs, FPS, and accuracy. Our proposed NEXT achieves the best performance with an mAP/Rank-1 of 82.4%/86.6%, while maintaining a moderate model size of 94.8M parameters. Compared to other MoE-based methods, such as DeMo (98.8M) and MFRNet (101.8M), NEXT reduces the parameter count by 4M and 7M, demonstrating higher efficiency. Although NEXT has slightly higher FLOPs (44.8G) than IDEA (43.7G), this is due to the use of the CLIP text encoder, denoted by *. However, it still remains significantly more efficient than MambaPro (52.4G). In terms of inference speed, NEXT achieves 275.1 FPS, which is slightly lower than IDEA (299.5), but outperforms MambaPro (243.2). These results validate that NEXT delivers state-of-the-art performance with an excellent trade-off between model complexity and efficiency.

C. Reliable Caption Generation

Thanks to the powerful semantic understanding capability of Multi-modal Large Language models (MLLMs), we can leverage their out-of-the-box ability to generate comprehensive textual semantic descriptions about the object appearance. However, simple template-based text generation methods (Wang et al. 2025c; Hu, Yang, and Ye 2024; Zhai et al. 2024) face many practical challenges when deal with multi-modal data, such as noise interference from low-quality images and significant style discrepancies in infrared modal-

Index	Modules			MSVR310				RGBNT201			
	MGFA	TMSE	CSSE	<i>mAP</i>	R-1	R-5	R-10	<i>mAP</i>	R-1	R-5	R-10
A	✗	✗	✗	50.1	68.9	83.4	87.8	71.0	73.6	84.2	88.2
B	✓	✗	✗	55.0	73.3	86.8	91.7	74.2	76.6	87.8	91.3
C	✓	✓	✗	59.7	75.1	88.2	92.0	78.9	84.4	91.1	93.2
D	✓	✓	✓	60.8	79.0	89.2	92.2	82.4	86.6	92.0	94.7

Table 6: Ablation studies of different modules on MSVR310 and RGBNT201.

Methods	Params (M)	FLOPs (G)	FPS	<i>mAP</i>	R-1
EDITOR (Zhang et al. 2024)	119.3	40.8	335.1	66.5	68.3
TOP-ReID (Wang et al. 2024)	324.5	35.5	398.9	72.3	76.6
ICPL-ReID* (Li et al. 2025)	45.4	39.8	358.4	75.1	77.4
PromptMA (Zhang et al. 2025)	107.9	36.2	343.5	78.4	80.9
DeMo (Wang et al. 2025b)	98.8	35.1	403.6	79.0	82.3
MambaPro (Wang et al. 2025a)	74.8	52.4	243.2	78.9	83.4
IDEA* (Wang et al. 2025c)	91.7	43.7	299.5	80.2	82.1
MFRNet (Feng et al. 2025)	101.8	33.3	391.7	80.7	83.6
NEXT(Ours)*	94.8	44.8	275.1	82.4	86.6

Table 7: Comparison with state-of-the-art methods on the size of learnable parameters, flops and fps on RGBNT201. * denotes the use of CLIP text encoder in inference stage.

Index	Router Type		Metrics	
	E_T	E_C	<i>mAP</i>	R-1
A	<i>Multi.</i>	<i>Multi.</i>	78.3	82.5
B	<i>Share.</i>	<i>Multi.</i>	78.7	83.4
C	<i>Share.</i>	<i>Share.</i>	80.3	84.3
D	<i>Multi.</i>	<i>Share.</i>	82.4	86.6

Table 8: Effectiveness of different routing strategies. *Multi.* means each modality uses a different router. *Share.* denotes all modalities use a shared router.

ities, making it difficult to obtain clear object textual descriptions. To this end, our proposed approach firstly employs multiple MLLMs to generate a set of attributes with confidence scores, and secondly we leverage the confidence scores with a multi-modal attributes aggregation strategy to generate reliable and comprehensive object identity appearance descriptions.

Confidence-Aware Attributes Generation

To flexibly analyze the appearance information of the object, we use the generation of identity attributes as the basic step of caption generation. We first define an instruction template to guide multiple MLLMs (*e.g.*, GPT-4o (Hurst et al. 2024), Qwen-VL (Bai et al. 2023), etc.) in structuring the attribute set of the input image. However, simple structured attribute information cannot quantitatively measure the confidence level of each item, the model suffers from low-quality

visual modality noise, which leads to incorrect attribute selection. To address this, we introduce the concept of **confidence** score in the instruction template (See Template. 14 and Template. 15 for the full attribute template.) This allows us to observe the confidence level of each MLLM assigns to its output for each attribute. Additionally, to avoid the model ignoring environment information, we not only structure the output of ‘age’, ‘gender’, ‘upper clothing’, ‘lower clothing’, ‘hairstyle’, ‘footwear’ and other appearance attributes (in the case of pedestrian), but also require the MLLMs to output ‘view’, ‘illumination’, ‘capture time’, and ‘target clarity’ attributes to aware environmental information.

Multi-Modal Attributes Aggregation

Based on the structured attribute set with confidence score, we are able to further generate reliable captions for the object. However, as shown in Fig. 2 (a) and Fig. 7, the RGB modal is affected by lighting degradation, causing the MLLMs to fail recognize the ‘backpack’ attribute. In contrast, the thermal infrared modality for the same identity easily reveals additional ‘backpack’ attribute. This leads to the model generating vague and incomplete textual captions such as ‘none’, ‘unknown’, or ‘unclear’ based on mono visual modality. To address this problem, we propose a multi-modal attribute aggregation strategy based on confidence scores to preprocess semantic complementary information in different visual modalities.

(1) Multi-Modal Merge and Complement. Specifically, we first use multiple MLLMs to identify object attributes, and for each identified attribute we select the MLLMs

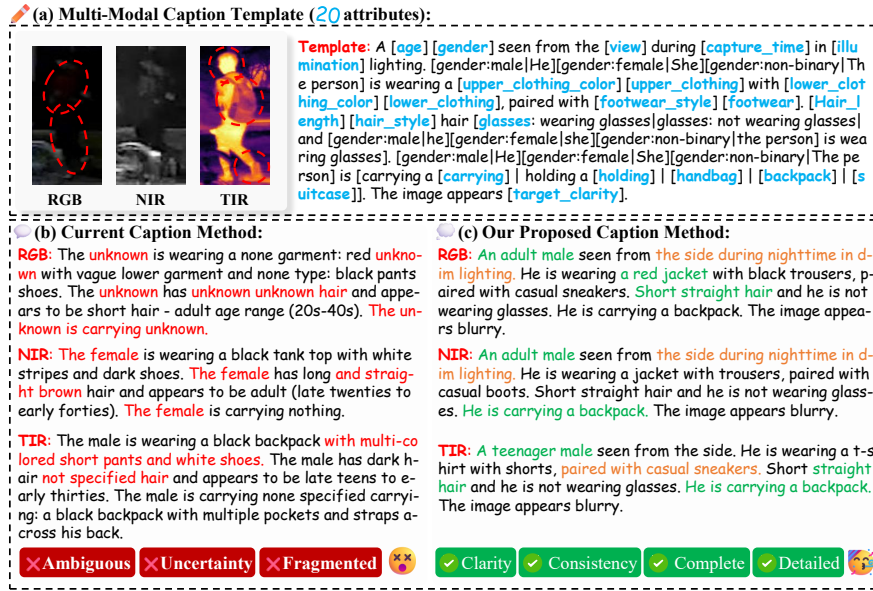


Figure 7: Generated caption samples and text quality analysis on RGBNT201 dataset.

with the highest confidence as their final value to improve the accuracy of each attribute within the modality. Furthermore, taking the RGB modality as an example, its modality-specific low-frequency attributes, such as ‘illumination,’ ‘upper clothing color,’ and ‘lower clothing color,’ are easy to recognize. In contrast, attributes requiring high-frequency information, such as ‘carrying,’ ‘holding,’ ‘handbag,’ and ‘backpack,’ are often incorrectly recognized as ‘unknown,’ ‘unclear,’ or ‘not carrying.’ This significantly affects the clarity of the final generated captions. To address this, we rely on the confidence scores to select the highest-confidence attributes from the NIR and TIR modalities, which are unaffected by lighting conditions, in order to recheck and complement the absent information. Similarly, we apply the same complementary strategy to each modality in order to obtain a complete and reliable set of attributes for each modality.

(2) Caption Generation. Building on the above complete attribute set, we define the following instruction template to guide the LLM (Liu et al. 2024a) in combining the structured attribute set from each modality to generate the final text caption (See Template. 16 and Template. 17 for the full caption template.) Finally, we have constructed a complete and reliable caption generation pipeline, and we leverage the same process on vehicle datasets to obtain a comprehensive semantic description of the vehicle.

D. Visualization Analysis

Expert Feature Visualization

As shown in Fig. 8 and Fig. 9, to further explore the recognition and perception capabilities of each expert, we visualize the sampled tokens of semantic experts and the activated regions of structural experts. Clearly, we observe that each semantic expert $\mathbf{E}_T = \{E_t^{(1)}, E_t^{(2)}, \dots, E_t^{(N_T)}\}$ tends to fo-

cus on tokens related to the target, which allows the experts to attend to distinct semantic parts. Moreover, each semantic expert preferentially samples tokens from different spectral modalities. The semantic experts effectively sample complementary tokens across modalities, demonstrating their ability to perceive fine-grained object parts and extract multi-modal features under text modulation. Furthermore, we observe that structural experts $\mathbf{E}_C = \{E_c^{(1)}, E_c^{(2)}, \dots, E_c^{(N_C)}\}$ consistently perceive the complete structure within modalities, maintaining coarse-grained structural features of the object. These visualizations strongly support the effectiveness of NEXT’s multi-grained expert design that models ReID through semantic sampling and structural perception.

Retrieval Results

To verify the model’s effectiveness in real world scenarios, we visualize the retrieval results of models with different module combinations on the RGBNT201 and MSVR310 datasets and compare NEXT with state-of-the-art methods. As shown in Fig. 10, on the RGBNT201 dataset, the introduction of different modules enables the model to more effectively recognize pedestrians with the same identity. Fig. 11 compares NEXT with existing state-of-the-art methods, demonstrating that our method achieves superior retrieval performance for target person under various low-light conditions. In Fig. 12, on the MSVR310 dataset, the model’s ability to identify challenging vehicles progressively improves with the addition of different components. Fig. 13 compares NEXT to current state-of-the-art methods, showing that our method effectively leverages multi-modal data to overcome challenges in low-light and cross-day-night scenarios, accurately identifying vehicles.

Multi-Modal Caption

RGB: An adult male seen from the side during nighttime in dim lighting. He is wearing a dark jacket with dark trousers, paired with casual boots. Short straight hair and he is not wearing glasses. He is carrying a backpack. The image appears blurry.

NIR: An adult male seen from the side during nighttime in dim lighting. He is wearing a jacket with trousers, paired with casual sneakers. Short hair and not wearing glasses. He is holding a phone. The image appears blurry.

TIR: A adult male seen from the side. He is wearing a jacket with trousers, paired with casual sneakers. Short straight hair and he is not wearing glasses. He is holding a phone. The image appears blurry.

RGB: An adult female seen from the side during nighttime in dim lighting. She is wearing an orange jacket with blue jeans, paired with athletic sneakers. Long hair and not wearing glasses. She is carrying a handbag. The image appears blurry.

NIR: An adult female seen from the side during nighttime in dim lighting. She is wearing a jacket with shorts, paired with casual sneakers. Medium straight hair and she is not wearing glasses. She is carrying a handbag. The image appears blurry.

TIR: An adult female seen from the side. She is wearing a jacket with trousers, paired with casual sneakers. Long straight hair and she is not wearing glasses. She is carrying a handbag. The image appears clear.

RGB: An adult female seen from the back during daytime in dim lighting. She is wearing a brown jacket with black trousers, paired with casual footwear. Medium straight hair and not wearing glasses. She is carrying a handbag. The image appears blurry.

NIR: An adult female seen from the side during daytime in bright lighting. She is wearing a jacket with trousers, paired with casual boots. Medium straight hair and she is not wearing glasses. She is carrying a handbag. The image appears blurry.

TIR: An adult male seen from the side. He is wearing a jacket with trousers, paired with casual sneakers. Short straight hair and he is not wearing glasses. He is carrying a handbag. The image appears blurry.

RGB: An adult female seen from the back during nighttime in dim lighting. She is wearing long straight hair and is not wearing glasses. She is holding a phone. The image appears blurry.

NIR: An adult male seen from the front during nighttime in dim lighting. He is wearing a t-shirt with trousers, paired with casual sneakers. Short straight hair and he is not wearing glasses. He is holding a phone. The image appears blurry.

TIR: An adult female seen from the front. She is wearing a long-sleeve shirt with trousers, paired with casual sneakers. Long straight hair and she is not wearing glasses. She is holding a phone. The image appears clear.

RGB: An adult male seen from the side during nighttime in dim lighting. He is wearing a black jacket with black trousers, paired with unknowable due to low clarity. Short unknowable due to low clarity hair and he is not wearing glasses. He is holding a phone. The image appears blurry.

NIR: An adult male seen from the side during nighttime in dim lighting. He is wearing a t-shirt with shorts, paired with casual sneakers. Short straight hair and he is not wearing glasses. He is holding a phone. The image appears blurry.

TIR: An adult male seen from the front. He is wearing a t-shirt with trousers, paired with casual sneakers. Short straight hair and he is not wearing glasses. He is holding a phone. The image appears clear.

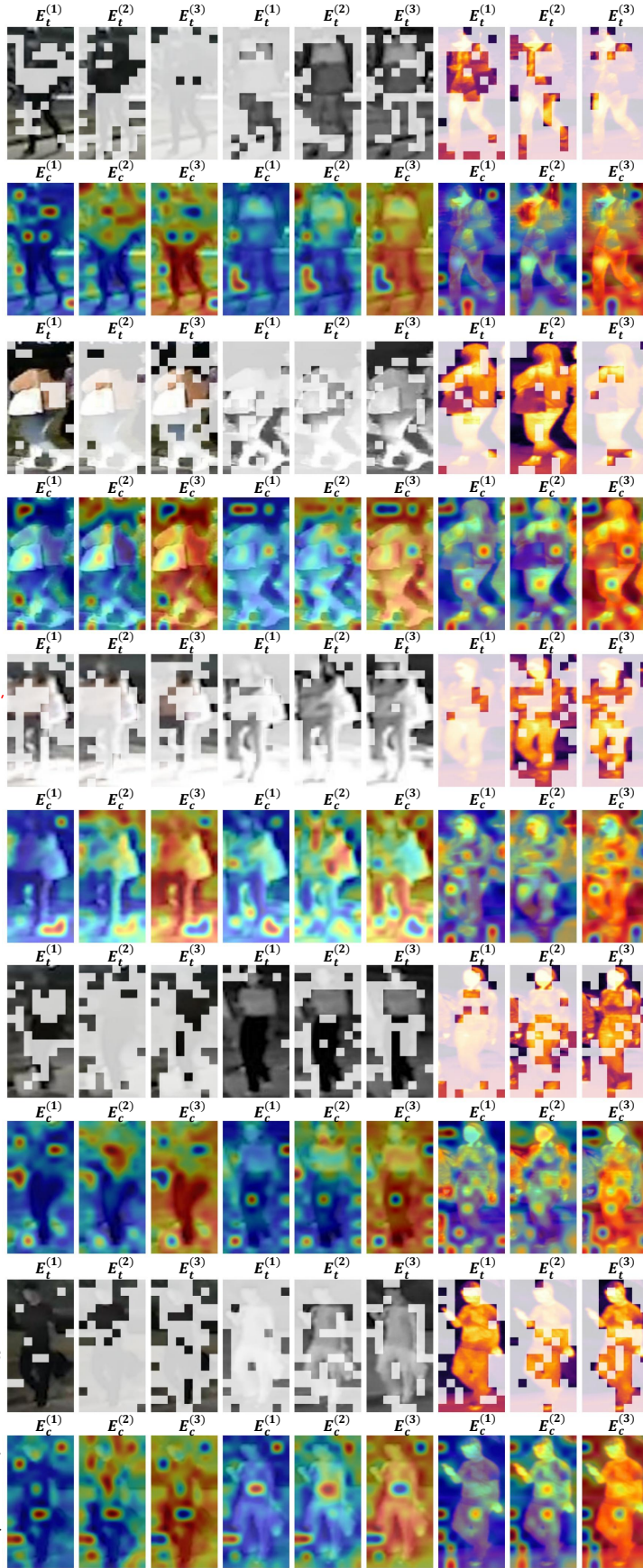


Figure 8: Visualization of the sampled patch tokens and activated feature regions for experts on RGBNT201.

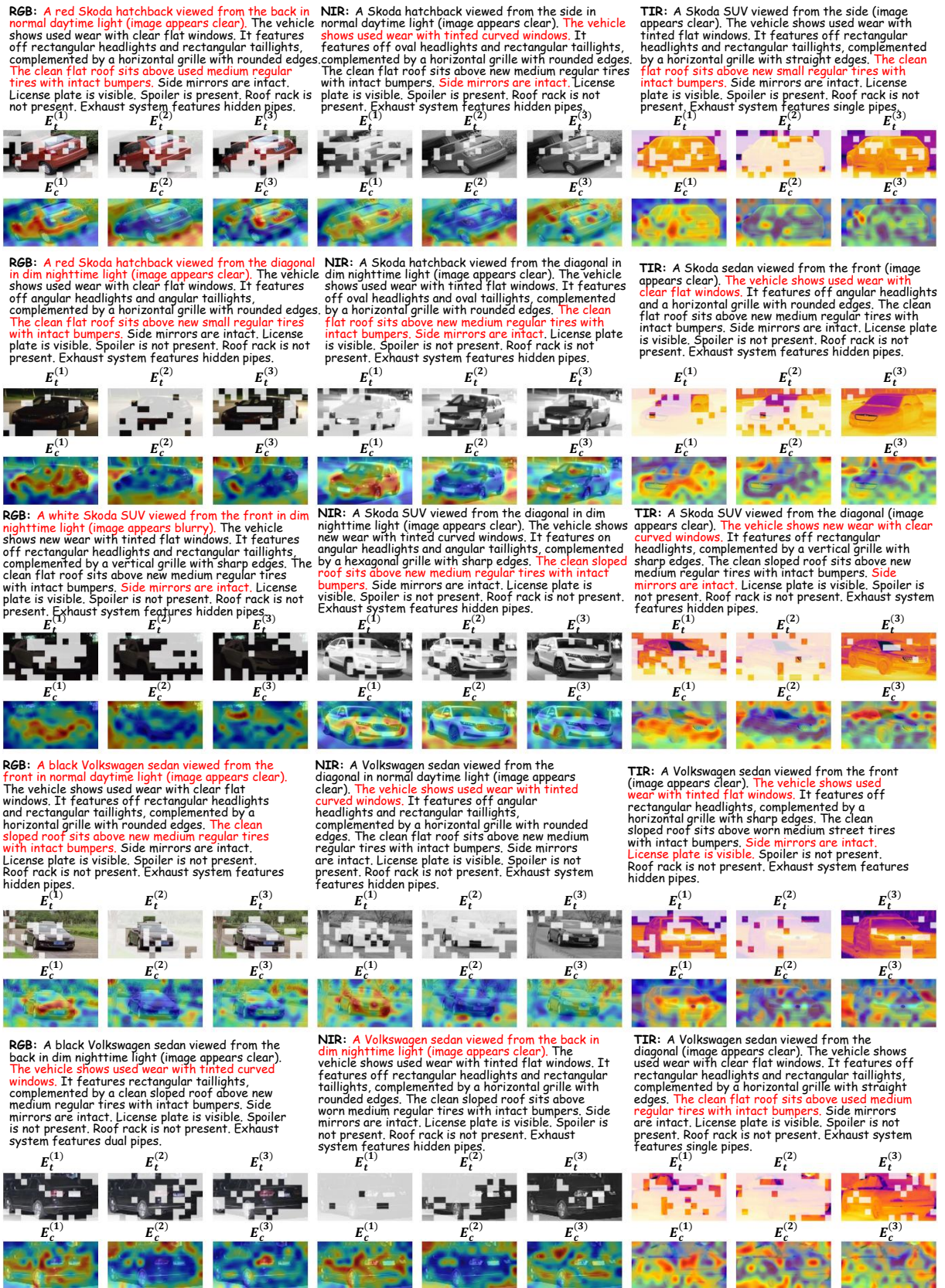


Figure 9: Visualization of the sampled patch tokens and activated feature regions for experts on MSVR310.

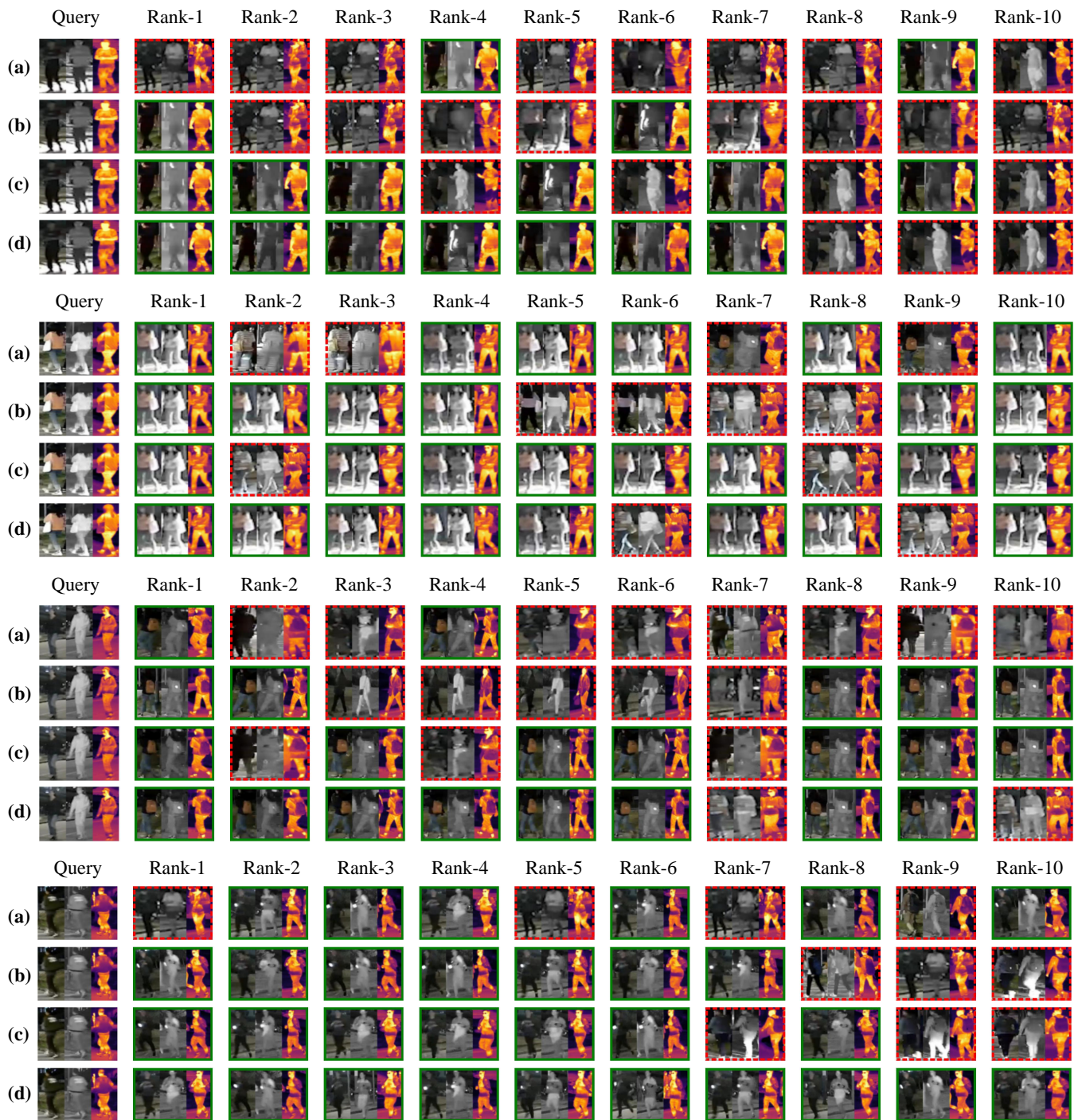


Figure 10: Visualization of the retrieval results on RGBNT201 (a) Baseline, (b) Baseline + MGFA, (c) Baseline + MGFA + TMSE, and (d) Baseline + MGFA + TMSE + CSSE (Ours).

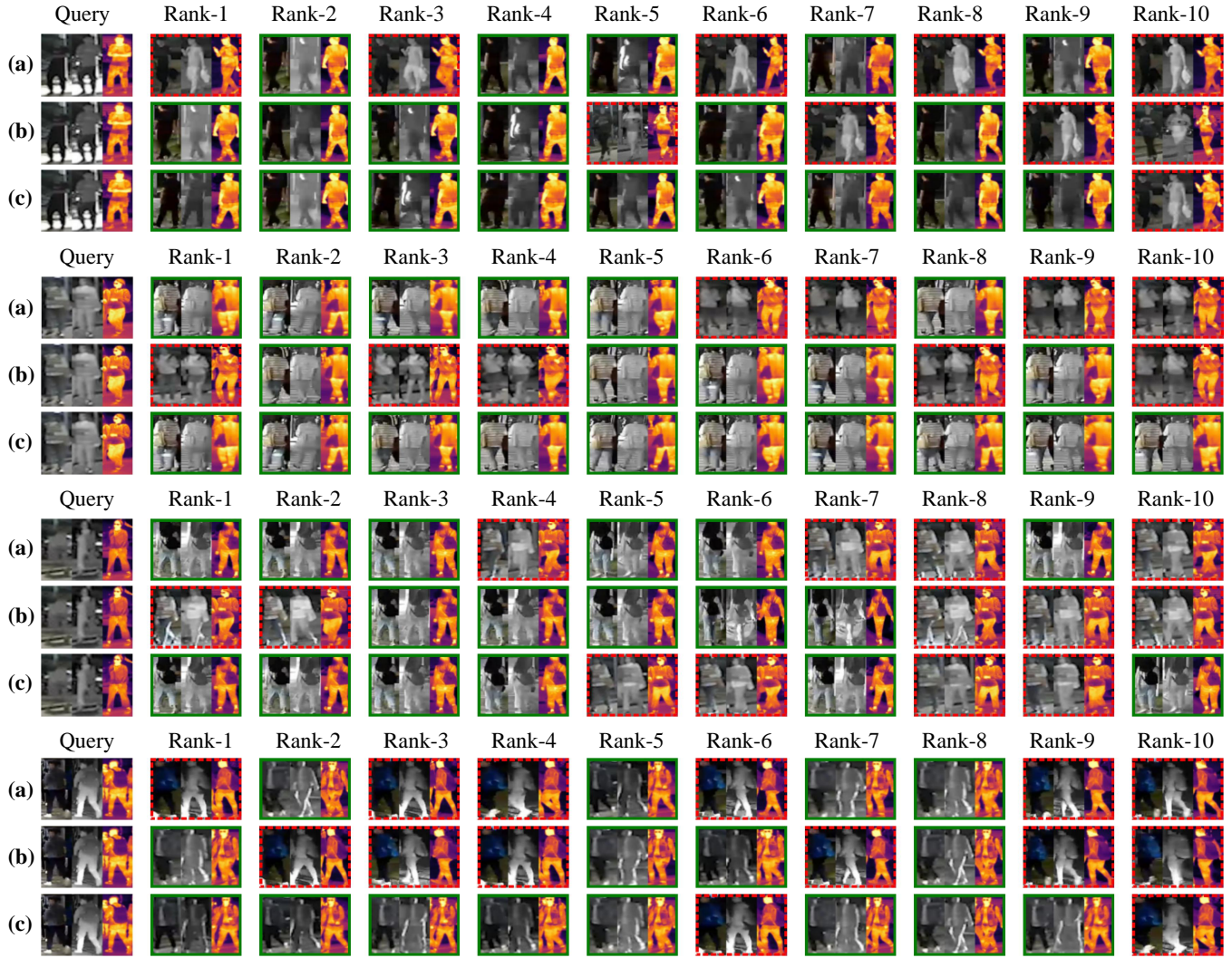


Figure 11: Visualization of the retrieval results on RGBNT201 (a) DeMo, (b) IDEA, and (c) NEXT (Ours).



Figure 12: Visualization of the retrieval results on MSVR310 (a) Baseline, (b) Baseline + MGFA, (c) Baseline + MGFA + TMSE, and (d) Baseline + MGFA + TMSE + CSSE (Ours).



Figure 13: Visualization of the retrieval results on MSVR310 (a) DeMo, (b) ICPL-ReID, and (c) NEXT (Ours).

Attribute Template (Person)

You are a visual analysis assistant specialized in processing images. Analyze the provided image and identify the most obvious person using the following attribute template. If the image is in visible light, include clothing color details. Output your result strictly as valid JSON. For each attribute, include a "value" (selected from the provided options or descriptive text), a "confidence" score between 0 and 1.

```
{
  "age": {"value": "child | teenager | adult | senior", "confidence": 0.0},
  "gender": {"value": "male | female | non-binary", "confidence": 0.0},
  "view": {"value": "front | back | side", "confidence": 0.0},
  "illumination": {"value": "bright | normal | dim", "confidence": 0.0},
  "capture_time": {"value": "daytime | nighttime | unclear", "confidence": 0.0},
  "target_clarity": {"value": "clear | blurry", "confidence": 0.0},
  "upper_clothing": {"value": "e.g., t-shirt | sweater | jacket", "confidence": 0.0},
  "upper_clothing_color": {"value": "e.g., red, blue, green", "confidence": 0.0},
  "lower_clothing": {"value": "e.g., jeans | shorts | skirt", "confidence": 0.0},
  "lower_clothing_color": {"value": "e.g., black, blue", "confidence": 0.0},
  "hair_length": {"value": "short | medium | long", "confidence": 0.0},
  "hair_style": {"value": "e.g., straight | curly", "confidence": 0.0},
  "footwear": {"value": "e.g., sneakers | sandals", "confidence": 0.0},
  "footwear_style": {"value": "e.g., casual | formal", "confidence": 0.0},
  "carrying": {"value": "e.g., backpack | luggage | none", "confidence": 0.0},
  "holding": {"value": "e.g., a phone | bottle | none", "confidence": 0.0},
  "handbag": {"value": "carrying handbag | not", "confidence": 0.0},
  "backpack": {"value": "carrying backpack | not", "confidence": 0.0},
  "glasses": {"value": "wearing glasses | not", "confidence": 0.0},
  "suitcase": {"value": "dragging | not dragging", "confidence": 0.0}
}
```

Please provide the analysis in valid JSON only.

Figure 14: Instruction template for generating person attributes with confidence.

Attribute Template (Vehicle)

You are a visual analysis assistant specialized in processing images. Analyze the provided image and identify the most obvious vehicle using the following attribute template. If the image is in visible light, include clothing color details. Output your result strictly as valid JSON. For each attribute, include a "value" (selected from the provided options or descriptive text), a "confidence" score between 0 and 1.

```
{
  "vehicle_type": {"value": "e.g., sedan | SUV | truck | coupe | convertible | minivan | hatchback | motorcycle, etc", "confidence": 0.0},
  "branding": {"value": "e.g., Volkswagen | Skoda | Mitsubishi | Mazda | Honda | Geely | Ford | Buick | BMW | Benz | Audi, etc", "confidence": 0.0},
  "color": {"value": "red | blue | black | white | silver | gray | yellow | green | orange | brown | purple", "confidence": 0.0},
  "view": {"value": "front | back | side | top | diagonal", "confidence": 0.0},
  "illumination": {"value": "bright | normal | dim", "confidence": 0.0},
  "capture_time": {"value": "daytime | nighttime | unclear", "confidence": 0.0},
  "target_clarity": {"value": "clear | blurry", "confidence": 0.0},
  "window_condition": {"value": "clear | tinted | broken | dirty | unclear", "confidence": 0.0},
  "window_style": {"value": "flat | curved | panoramic", "confidence": 0.0},
  "exterior_condition": {"value": "new | used | worn | damaged", "confidence": 0.0},
  "headlights_shape": {"value": "round | oval | rectangular | angular", "confidence": 0.0},
  "taillights_shape": {"value": "round | oval | rectangular | angular", "confidence": 0.0},
  "front_grille_shape": {"value": "horizontal | vertical | hexagonal | angular", "confidence": 0.0},
  "front_grille_edges": {"value": "sharp | rounded | straight | irregular", "confidence": 0.0},
  "roof_type": {"value": "flat | sloped | sunroof | convertible | dome", "confidence": 0.0},
  "roof_condition": {"value": "clean | dirty | damaged", "confidence": 0.0},
  "tires_type": {"value": "all-terrain | street | off-road | winter | regular", "confidence": 0.0},
  "tires_condition": {"value": "new | worn | damaged", "confidence": 0.0},
  "tire_size": {"value": "small | medium | large", "confidence": 0.0},
  "headlights_condition": {"value": "on | off | dimmed | broken", "confidence": 0.0},
  "bumper_condition": {"value": "intact | damaged | missing", "confidence": 0.0},
  "license_plate": {"value": "visible | not visible", "confidence": 0.0},
  "spoiler": {"value": "present | not present", "confidence": 0.0},
  "roof_rack": {"value": "present | not present", "confidence": 0.0},
  "side_mirrors": {"value": "present | not present", "confidence": 0.0},
  "side_mirror_condition": {"value": "intact | broken | missing", "confidence": 0.0},
  "exhaust_type": {"value": "single | dual | hidden", "confidence": 0.0}
}
```

Please provide the analysis in valid JSON only.

Figure 15: Instruction template for generating vehicle attributes with confidence.

Caption Template (Person):

Generate a natural person appearance description by strictly following this template and using ONLY the highest-confidence attributes from the provided JSON data (ignore any with 0 confidence).

'A [age] [gender] seen from the [view] during [capture_time] in [illumination] lighting. [gender:male|He][gender:female|She][gender:non-binary|The person] is wearing a [upper_clothing_color] [upper_clothing] with [lower_clothing_color] [lower_clothing], paired with [footwear_style] [footwear]. [Hair_length] [hair_style] hair [glasses: wearing glasses|glasses: not wearing glasses] and [gender:male|he][gender:female|she][gender:non-binary|the person] is wearing glasses. [gender:male|He][gender:female|She][gender:non-binary|The person] is [carrying a [carrying] | holding a [holding] | [handbag] | [backpack] | [suitcase]]. The image appears [target_clarity].'

Do not include any introductory text, titles, explanations, or content outside this template structure.

Figure 16: Instruction template for generating person caption.

Caption Template (Vehicle):

Generate a natural vehicle appearance description by strictly following this template. Always use highest-confidence values from these two JSON datasets of the same vehicle (ignore confidence=0).

'A [color] [branding] [vehicle_type] viewed from the [view] in [illumination] [capture_time] light (image appears [target_clarity]). The vehicle shows [exterior_condition] wear with [window_condition] [window_style] windows. It features [headlights_condition] [headlights_shape] headlights and [taillights_shape] taillights, complemented by a [front_grille_shape] grille with [front_grille_edges] edges. The [roof_condition] [roof_type] roof sits above [tires_condition] [tire_size] [tires_type] tires with [bumper_condition] bumpers. [Side mirrors are [side_mirror_condition].] [License plate is [license_plate].] [Spoiler is [spoiler].] [Roof rack is [roof_rack].] [Exhaust system features [exhaust_type] pipes.]'

Omit any bracketed sections where data is unavailable. Do not include any introductory text, titles, explanations, or content outside this template structure.

Figure 17: Instruction template for generating vehicle caption.